Journal of Photochemistry & Photobiology, B: Biology 191 (2019) 99–106

Contents lists available at ScienceDirect

Journal of Photochemistry & Photobiology, B: Biology

journal homepage: www.elsevier.com/locate/jphotobiol

FRET-based dual channel fluorescent probe for detecting endogenous/exogenous H_2O_2/H_2S formation through multicolor images

Nithya Velusamy[a,1], Natesan Thirumalaivasan[b,1], Kondapa Naidu Bobba[a], Arup Podder[a], Shu-Pao Wu[b,*], Sankarprasad Bhuniya[a,c,**]

[a] Amrita Centre for Industrial Research & Innovation, Amrita School of engineering, Coimbatore Amrita University, 64112, India
[b] Department of Applied Chemistry, National Chiao Tung University, 1001 Ta Hsueh Road, Hsinchu 300, Taiwan
[c] Department of Chemical Engineering & Materials Science, Amrita School of Engineering, Coimbatore, Amrita Vishwa Vidyapeetham, Amrita University, 641112, India

ARTICLE INFO

Keywords:
FRET- based fluorescent probe
Coumarin
Naphthalimide
Endogenous H_2O_2
Endogenous H_2S

ABSTRACT

We have developed a FRET-based fluorescent probe (**PHS1**) as a combination of two different fluorophores (coumarin and naphthalimide); which can detect both exogenous and endogenous H_2S and H_2O_2 in live cells through multicolor images. The precise overlap between UV-absorption of naphthalimide and the emission band of coumarin in probe **PHS1** allows the acquisition of the self-calibrated information of dual analytes through FRET-based imaging. The UV–Vis absorption (λ_{abs} 390 nm) and fluorescence emission (λ_{em} 460 nm) of probe **PHS1** in the presence of H_2O_2 are increased ∽35- fold and ∽15-fold respectively. It also allows the estimation of the levels of H_2S through enhancement of emission intensity at 550 nm. The probe **PHS1** exhibits high stability against various analytes, including various pH (4–9.5). The cell viability assay data indicate that the probe is not harmful to the cancer cells. The nontoxic nature of the probe **PHS1** encourages application for cancer cell labeling. The probe **PHS1** can detect the level of endogenous H_2O_2, H_2S, and H_2O_2/H_2S in cancer cells through blue, green and FRET-based green channel imaging. **PHS1** is a unique probe, has potential application for diagnosing cancer by providing information on the level of dual analytes (H_2S, H_2O_2) in cancer cells.

1. Introduction

Hydrogen peroxide (H_2O_2) and hydrogen sulfide (H_2S) are endogenously produced small reactive molecular species. Those have a significant role in physiological and pathological consequences in living organisms [1–4]. In physiological condition, they play a pivotal role in redox signaling pathway [5]. Depending on their concentrations and locations they exhibit pro- or anti-apoptotic activities and behave like a double-edged sword in cancer prognosis [6,7]. H_2O_2 is a crucial ROS produced in the mitochondrial respiratory chain cascade. It participates in various physiological processes, namely, cell proliferation and differentiation, and also in hypoxia signal transduction [8]. In cancer cells, the anaerobic glycolysis process predominantly produces superoxide anion (O_2^-); which rapidly reacts with appropriate superoxide dismutase to generate H_2O_2. This ROS deactivates functions of tumor suppressor gene p53 and activates several oncogenic pathways such as RAS, MYC, and AKT to accelerate tumor progression [9,10]. On the other hand, hydrogen sulfide (H_2S) as the third gasotransmitter plays a significant role in several physiological processes, including cardiovascular, gastrointestinal, immune defense, and nervous systems [11,12]. Indeed, it supports tumor growth via stimulating the angiogenesis, regulating mitochondrial bioenergetics, stimulation of cell cycle progression and anti-apoptosis function [13]. Apart from cancer, irregular production of endogenous H_2S is associated with numerous diseases such as Alzheimer's disease, Down syndrome, diabetes, and liver cirrhosis [14–17]. The enzymes cystathionine-β-synthase (CBS) and cystathionine-γ-lyase (CSE) are mainly responsible for overproduction of H_2S in cancer cells [18]. Moreover, CBS induces oxidative stress. Taking advantage of fluorescence modality, several fluorescent probes have been developed to expose and visualize various biological events through fluorescence imaging in vitro as well as in vivo [19–27]. In the present decade, several fluorescent probes have visualized both endogenous and exogenous H_2O_2 [28–35] and H_2S [36–45] formation in vitro and within live-specimens. Chang and his co-worker observed that NADPH-oxidase derived H_2O_2 stimulate endogenous H_2S formation in human umbilical vein endothelial cells [46]. Thus, we are

* Corresponding author.
** Corresponding author at: Amrita Centre for Industrial Research & Innovation, Amrita School of engineering, Coimbatore Amrita University, 64112, India.
E-mail addresses: spwu@mail.nctu.edu.tw (S.-P. Wu), b_sankarprasad@cb.amrita.edu (S. Bhuniya).
[1] These authors equally contributed to this study.

https://doi.org/10.1016/j.jphotobiol.2018.12.016
Received 9 October 2018; Received in revised form 18 December 2018; Accepted 19 December 2018
Available online 26 December 2018
1011-1344/

interested in developing FRET-based ratiometric fluorescent probes to detect H_2O_2, H_2S, and the combination of them (H_2O_2/H_2S) in cancer cells; the early information on H_2O_2/H_2S can help in diagnosing cancer and open a new research avenue for tracking of cancer cells. Moreover, this dual sensing strategy simultaneously can provide information on two different analytes (H_2O_2/H_2S), and their intracellular location through dual-channel imaging.

2. Experimental Procedures

2.1. General Information on Materials, Methods and Instrumentations

Diethylmalonate (Avra, India), 2,4-dihydroxy-3-methylbenzaldehyde (Alfa Aesar, India), piperidine (Avra, India), bromo-1,8-naphthalic anhydride (TCI, Japan), ethanol (Changshu Yangyuvan Chemical, China), ethylenediamine (Sigma Aldrich, India), sodium azide (Loba Chem, India), DMSO (Loba Chem, India), lithium hydroxide (Himedia, India), N-Phenyl-bis(trifluoromethanesulfonimide) (Avra, India), bis (pinacolato)diboron (Avra, India), 1,1′-Bis(diphenylphosphino) ferrocene dichloropalladium (II) complex with dichloromethane (Avra, India), N-(3-dimethylaminopropyl)-N′-ethylcarbodiimide hydrochloride (Avra, India), hydroxybenzotriazole hydrate (Himedia, India), sodium carbonate (Himedia, India), THF (Merck, India), DMF (Avra, India), potassium acetate (Himedia, India), toluene (Avra, India), 4- and sodium sulfate (Loba Chem, India) were procured from commercial sources and used as such. In column chromatography silica gel (100–200 mesh, Loba Chem) was used as the stationary phase. Shimadzu UV-1800 spectrophotometer was used for recording UV–Vis. spectra. NMR spectra were taken on a 400 MHz spectrometer (Bruker, Germany). Mass spectra were collected on IonSpec HiResESI mass spectrometer.

2.2. Synthesis of *PHS1*

2.2.1. Synthesis of *1*

The compound **1** was prepared as per the previous report [47]. Diethyl malonate (1.263 g, 7.892 mmol) and piperidine (1.680 g, 19.731 mmol) were added to a solution of 2, 4-dihydroxy-3-methyl benzaldehyde (1.0 g, 6.577 mmol) in ethanol (20 mL). The reaction was continued for 12 h. Next, ethanol was evaporated. The residue was dissolved in HCl (2 N) and extracted with ethyl acetate. The organic layer was washed with water, brine and dried over anhydrous sodium sulfate. Then, it was concentrated under reduced pressure to get compound **1** as pale pink colour solid (1.25 g, 76.64%).

2.2.2. Synthesis of *2*

Compound **2** was prepared according to reported article [47]. The compound **1** (400 mg, 1.6125 mmol) was dissolved in DMF, *N*-phenyl-bis (trifluoromethyl sulphonamide) (1.1513 g, 3.22 mmol) and Na_2CO_3 (0.854 g, 8.062 mmol) were added and stirred overnight at rt. Then cold water was added and stirred for another 5 min to get a solid precipitate. The solid was filtered, dissolved in DCM and dried over anhydrous sodium sulfate. The crude compound was subjected to column chromatography to obtain **2** as a pink solid (0.375 g, 61.20%).

2.2.3. Synthesis of *3*

To a solution of **2** (2 g, 5.2629 mmol) in toluene (15 mL), bis(pinacol)diboron (1.736 g, 6.8412 mmol) and potassium acetate (1.547 g, 15.789 mmol) were added and purged with nitrogen gas for 15–20 min. Then, Pd(dppf)Cl_2 (1.289 g, 1.578 mmol) was added to the solution; further, purged with nitrogen gas for another 10 min. Following this, the reaction mixture was stirred at 110 °C for 2 h. The toluene was evaporated and compound was extracted with ethyl acetate. The organic layer was dried over anhydrous sodium sulfate. Finally, crude product was purified by silica gel column chromatography to afford a pale pink solid. ^{1}H NMR (400 MHz, DMSO-d_6): δ 8.704 (s, 1H), 7.576 (d, 2H, J = 6.0 Hz), 4.297 (q, 2H, J = 5.6 Hz), 2.496 (s, 3H), 1.315 (s, 15 Hz). ^{13}C NMR (100 MHz, DMSO-d_6). 12.82, 21.50, 97.54, 111.21, 117.62, 125.02, 126.98, 127.09, 127.44, 128.95, 129.48, 130.46, 135.91, 136.43, 145.52, 152.69, 152.87, 169.26, 172.42. ESI- HRMS m/z (M + H+): calcd. 359.1588, found 359.1666.

2.2.4. Synthesis of *4*

To compound **3** (600 mg, 2.30 mmol) in aqueous THF (10.0 mL), LiOH (320 mg) was added and stirred for 1 h. After completion of reaction, pH was adjusted to ∽5 using HCl (2.0 N) and then diluted with ethyl acetate. The combined organic layers were washed with water and brine. It was then dried over anhydrous sodium sulfate and evaporated under reduced pressure to afford compound **4** as pale yellow solid (340 mg, 69.16%). ^{1}H NMR (400 MHz, DMSO-d_6): δ 8.655 (s, 1H),7.281 (t, 1H, J = 6.01 Hz), 6.909 (d, 1H, J = 6.80 Hz), 2.365 (s, 3H), 1.320 (s, 12H). ^{13}C NMR (100 MHz, DMSO-d_6)0.14.32, 25.42, 84.56, 113.37, 124.84, 127.04, 131.49, 135.75, 148.49, 153.25, 158.37, 164.74. ESI- HRMS m/z (M + Na+): calcd. 353.1165, found 353.1162.

2.2.5. Synthesis of *A*

The compound **A** was synthesized according to the literature [48].

2.2.6. Synthesis of *PHS1*

HOBT (76 mg, 0.545 mmol) and EDCI (110 mg, 0.545 mmol) were added to a solution of **4** (180 mg, 0.542 mmol) in DMF and stirred for 15 min at RT. Then, **A** (184 mg, 0.654 mmol) was added to the reaction mixture. The reaction mixture was stirred overnight 50 °C and then poured into water (10 mL). The precipitated was filtered, washed with water, and dried under a vacuum; finally, it was purified by column chromatography (DCM/MeOH: 15/1) to get 150 mg of compound **PHS1** as a yellow solid. Yield: 46.38%. ^{1}H NMR (DMSO-d_6): 9.04 (s, 1H), 8.825 (d, 1H, J = 12.00 Hz), 8.639 (m, 2H), 8.435 (dd, 1H), 7.714 (m, 2H), 7.449 (m, 3H), 4.519 (t, 2H, J = 5.60 Hz), 3.888 (q, 2H), 2.653 (s, 2H), 2.468 (s, 1H), 1.371 (s, 12H). ^{13}C NMR (100 MHz, DMSO-d_6) 0.14.84, 18.88, 24.61, 24.96, 27.22, 30.12, 71.16, 73.54, 84.12, 115.99, 118.12, 118.68, 122.42, 123.61, 124.69, 125.09, 127.33, 128.33, 128.70, 131.50, 131.73, 135.08, 142.82, 147.58, 152.18, 159.88, 161.69, 162.33, 163.15, 163.58, 179.28. ESI- HRMS m/z (M + H+): calcd. 594.2082, found 594.2119, (M + Na+): calcd. 616.1979, found 616.2106.

2.3. UV/Vis and Fluorescence Spectroscopy

All fluorescence and UV–Vis. spectra were obtained with RF- 6000 FL spectrometer with a 1 cm standard quartz cell and UV-1800 spectrophotometer, respectively. Sodium sulfide (Na_2S) was used as the source of H_2S and H_2O_2 was used directly. Stock solutions (600 μM) of various analytes (HOCl, H_2O_2, $NaNO_2$, $Cu(OAc)_2$, $Zn(OAc)_2$, $Na_2S_2O_3$, $FeSO_4$, NO, KCl, $CaCl_2$, GSH, ascorbic acid (AA), cysteine, folic Acid, histidine, lysine, NaOCl, K_2S_5 were prepared in double distilled water. The stock solution of probe **PHS1** (40 μM) was prepared in PBS buffer (pH = 7.4) with 1% DMSO. Excitation was effected at 400 nm and 450 nm with excitation and emission slit widths as 5 nm each. The fluorescence experiments (solution test) of **PHS1** (10.0 μM) were recorded in the presence of increasing concentrations of H_2O_2 (0–25 eq.) and Na_2S (0–25 eq.) in HEPES buffer (pH = 7.4) with 1% DMSO. **PHS1** was incubated with Na_2S and H_2O_2 for 30 min at 37 °C.

2.4. Cytotoxicity Assay

By using methyl thiazolyl tetrazolium (MTT) assay, cellular cytotoxicity of **PHS1** in HT-29 cells was estimated. Several concentrations (0–50 μM) of **PHS1** were added to the wells of the HT-29 cells grown in a 96-well cell culture plate. Then the cells were maintained under 5% CO_2 at 37 °C under for 24 h. Subsequently, to each well 10 mL MTT

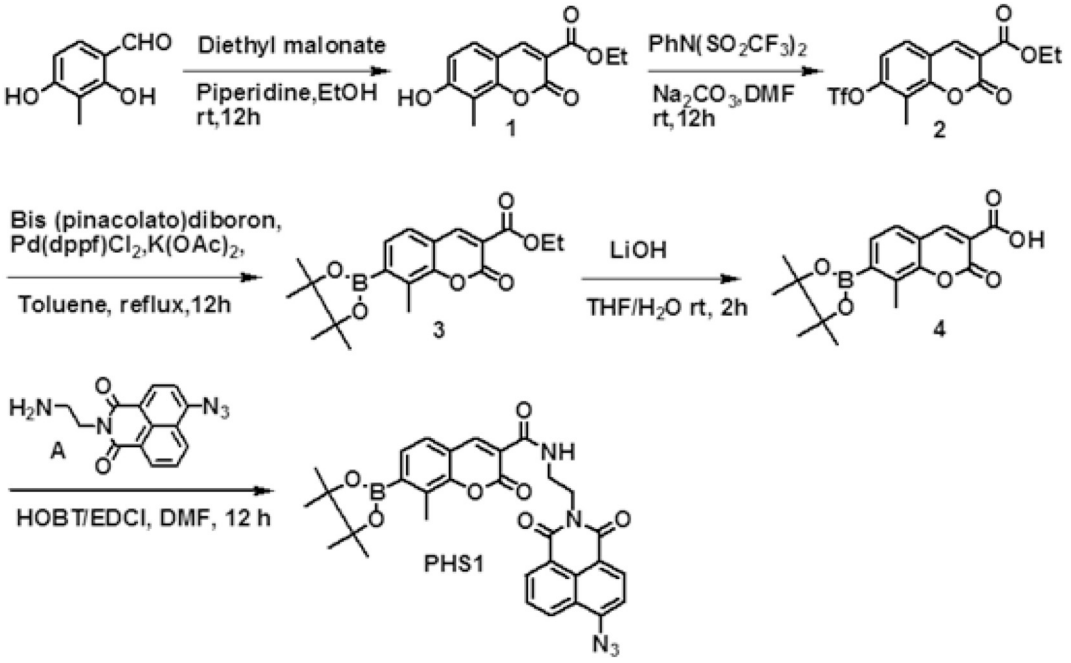

Scheme 1. Synthesis of probe **PHS1**.

(5 mg mL^{-1}) was added and incubated at 37 °C under 5% CO_2 for 4 h. Afterward, the MTT solution was removed and the yellow precipitates (formazan) were dissolved in 200 mL DMSO and 25 mL sorensen's glycine buffer (0.1 M glycine and 0.1 M NaCl). The absorbance of each well at 570 nm was measured using Mullikan GO microplate reader. By using the following equation the cell viability was calculated: Cell viability (%) = (Mean of absorbance values of treatment group)/(Mean of absorbance values of control group).

2.5. Cell Culture and Confocal Fluorescence Imaging for Endogenous H_2O_2 and H_2S in Living Cells

The HT-29 cells and HeLa cells were received from the Food Industry Research and Development Institute (Taiwan). The HT-29 and HeLa cell line were grown in McCoy's 5A and DMEM Medium with 10% (*v*/v) FBS (fetal bovine serum) and penicillin/streptomycin (100 μg mL-1) at 37 °C in a 5% CO_2 incubator respectively. The endogenous H_2S deduction was optimized through the HT-29 cells, which are treated with 10 μM of **PHS1** in DMSO and incubated for 1.30 h at 37 °C. The green fluorescence in cells increased significantly, indicating the generation of endogenous H_2S within the cells. Also, for endogenous H_2O_2 deduction in the HeLa cells, we incubated with PMA (25 ng mL^{-1}) for 2 h and then **PHS1** (10 μM) for 30 min at 37 °C. The culture medium was removed, and the treated cells were washed with 0.1 M PBS (2 mL × 3) before observation. The fluorescence images of cells were collected with a Leica TCS SP5 X AOBS Confocal Fluorescence Microscope (Germany) fitted with a 63 oil-immersion objective lens. The emissions bands were varied from 460 nm and 550 nm ± 10 nm respectively.

2.6. Confocal Fluorescence Imaging for Exogenous H_2O_2 in HeLa Cells

Cells were cultured in Dulbecco's modified Eagle's medium (DMEM) supplemented with 10% fetal bovine serum (FBS) at 37 °C under 5% CO_2 atmosphere. After 24 h, the cells were washed with PBS and then incubated with 10 μM of **PHS1** in 2 mL DMEM for 30 min. Then, H_2O_2 (150 μM) was added in culture media and incubated for 30 min. The culture medium was replaced, and the treated cells were washed with 0.1 M PBS (2 mL × 3). The fluorescence images of cells were acquired with the Leica TCS SP5 X AOBS Confocal Fluorescence Microscope (Germany). The excitation and emission wavelength were set at 410 nm/420–470 nm respectively.

2.7. FRET Imaging of Exogenous H_2O_2 and H_2S in HeLa Cells

As mentioned above, the cells were cultured in appropriate culture media. The probe **PHS1** (10 μM) were incubated with cells for 30 min. The treated cells were washed with PBS three times. Then, the cells were co-incubated with H_2O_2 (200 μM) and H_2S (200 μM) 30 min, the culture media were removed and washed with PBS-buffer. Leica TCS SP5 X AOBS Confocal Fluorescence Microscope (Germany) with a 63× oil-immersion objective lens was used for fluorescence imaging. Cell images were collected from the blue channel (450–480 nm) and green channel (540–580 nm) at the excitation wavelength 400 nm.

2.8. Zebrafish Imaging

The zebrafish were used as per the instructions of the National Institute of Health Taiwan, and acceptance of the Institutional Animal Care and Use Committee (IACUC) of National Chiao Tung University. The treatment of the zebrafish was done according to the direction for Animal Care and Use Committee of National Chiao Tung University. The zebrafish were maintained at an optimal breeding condition of around 28 °C. Under a 14 h light/10 h dark cycle, two male and female zebra fish were maintained in one tank at 28 °C for mating. The next morning, the laid eggs were triggered by light stimulation. After immediate fertilization of most of the eggs, the zebrafish were cultured in embryo medium (5 mL) with added 1-phenyl-2-thiourea (PTU) in 6-well plates for 24 h at ambient temperature. Immediately, the anesthetized (50 mg L-1 tricaine) zebrafish embryos were incubated with H_2S and H_2O_2 separately in E3 media for 30 min at ambient temperature. Several PBS washes removed the excess H_2S and H_2O_2 and then zebrafish were additionally incubated with **PHS1** (50 μM) for 30 min. Subsequent washes with PBS were done to remove the surplus probe and then the imaging of zebrafish was done using a Leica TCS SP5 X AOBS Confocal Fluorescence Microscope.

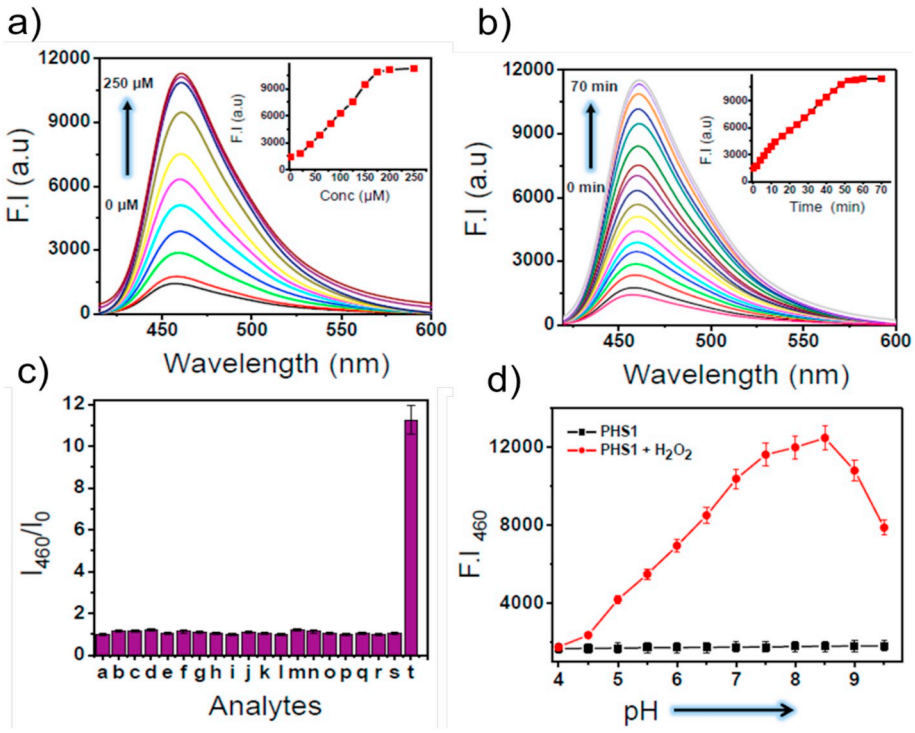

Fig. 1. (a) Fluorescence spectra of **PHS1** (10 μM) with H_2O_2 (0–250 μM). Inset: Average fluorescence intensity (λem = 460 nm) changes with H_2O_2. b) Fluorescence response of **PHS1** (10 μM) with H_2O_2 (200 μM) at time (0–70 min). c) Fluorescence response of **PHS1** (10 μM) towards 200 μM a: HOCl, b: Na_2S. c: $NaNO_2$, d: Tyrosinase, e: $Zn(OAc)_2$, f: $Na_2S_2O_3$, g: $FeSO_4$, h:NO i:Trypsin j: Pepsin k: Na_2CO_3, l: GSH (1 mM), m: Ascorbic Acid (1 mM), n: Cysteine (1 mM), o: Folic Acid (1 mM), p: Histidine (1 mM), q: Lysine (1 mM), r: NaOCl s: K_2S_5 and t: H_2O_2. d) Average fluorescence intensity changes of **PHS1** (10 μM) at λex = 390 nm in presence and absence of H_2O_2, (200 μM) at various pH (4–9.5). All the experiments were carried out in PBS buffer (pH = 7.4; 1% DMSO) at 37 °C with excitation at 390 nm and slit width set at 5 nm.

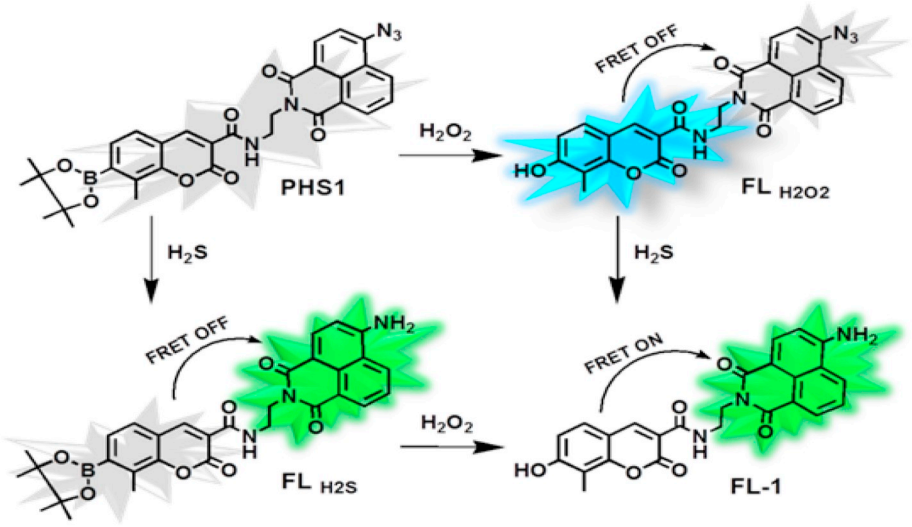

Scheme 2. Reaction mechanism of **PHS1** with H_2O_2, H_2S and H_2O_2/H_2S.

3. Results and Discussions

3.1. Synthesis and Photophysical Properties of *PHS1*

We synthesized probe **PHS1** as outlined in Scheme 1. All the intermediates and probe **PHS1** were characterized by ^{1}H NMR, ^{13}C and MS analysis (ESI†). The detail of the synthetic procedure and the spectroscopic information is available in the experimental section. In this design strategy, we have chosen coumarin and naphthalimide as the fluorophore because their distinct absorption in 390 and 460 nm (Fig. S1) can separate analytes H_2O_2 and H_2S respectively. Moreover, emission maxima for coumarin and naphthalimide fluorophore also have a distinctive range of 450 nm and 550 nm (Fig. S2) respectively; thereby, the two mentioned analytes can be detected selectively without any interferences. By introducing two fluorophores in **PHS1**, it is possible to acquire dual-colour images in living cells for the analytes H_2O_2 and H_2S respectively. Further, the overlap of the emission band of coumarin moiety with the absorption of naphthalimide (Fig. S3) has suggested that **PHS1** can provide information on temporal crosstalk between H_2O_2 and H_2S in living cells through FRET-based fluorescence imaging. Based on the above design strategy, 2we believe that **PHS1** could provide information on H_2O_2, H_2S, and H_2O_2/H_2S.

We then incubated **PHS1** with H_2O_2 (200.0 μM) for 1 h to know the UV-abs. Changes of **PHS1**. As we noticed in the Fig. S4, UV-abs. at 390 nm has 35-fold enhanced. Next, we titrated **PHS1** with variable concentrations of H_2O_2 (0–200.0 μM), as depicted in Fig. 1a, the fluorescence intensity at λ_{em} 460 nm is continuously increased with the increasing levels of H_2O_2. From the regression equation, obtained detection limit towards H_2O_2 was 12.1 × 10^{-5} μM (Fig. S5). The result of time-dependent (Fig. 1b) titration of **PHS1** with H_2O_2 indicated that 7-pinacolboronyl- coumarin moiety in **PHS1** was fully converted to 7-hydroxy coumarin derivative **FL_{H2O2}** within 60 min [8] (Scheme 2, Fig.

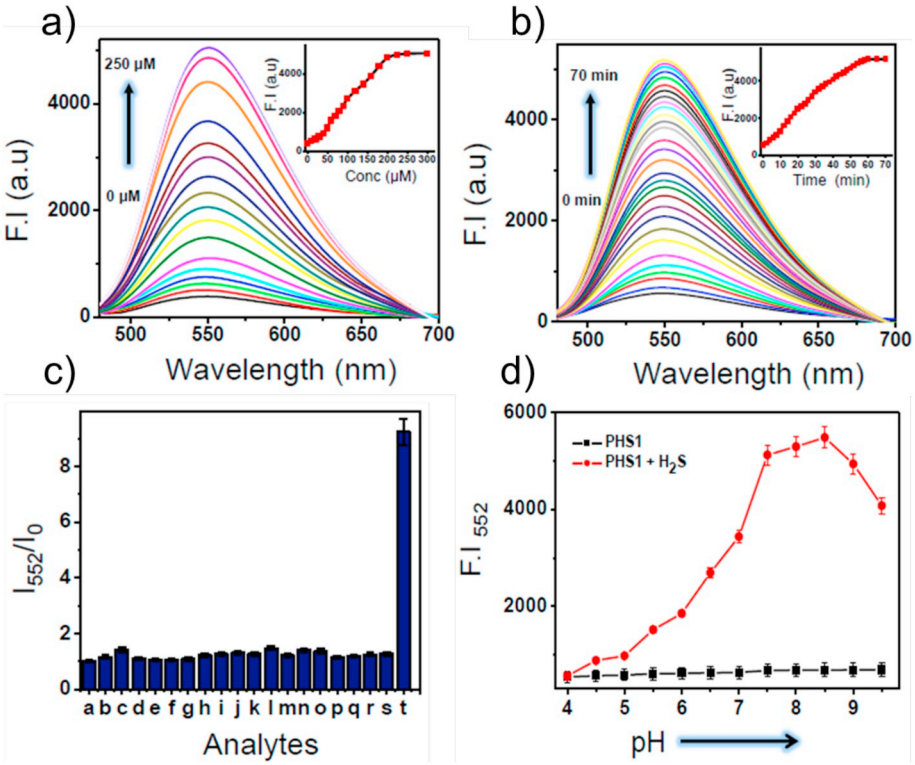

Fig. 2. a) Concentration dependent study of **PHS1** (10 μM) with Na_2S (0–250 μM). Inset: Concentration vs average fluorescence intensity (λem = 550). b) Fluorescence response of **PHS1** (10 μM) with Na_2S (200 μM) at time (0–70 min). c) Fluorescence response of **PHS1** (10 μM) towards 200 μM a: HOCl, b: H_2O_2, c: $NaNO_2$, d: Tyrosinase, e: $Zn(OAc)_2$, f: $Na_2S_2O_3$, g: $FeSO_4$, h:NO i: Trypsin j: Pepsin k: Na_2CO_3, l: GSH (1 mM), m: Ascorbic Acid (1 mM), n: Cysteine (1 mM), o: ALP (1 mM), p: Histidine (1 mM), q: Lysine (1 mM), r: NaOCl s: K_2S_5 and t: Na_2S. d) Average fluorescence intensity changes of **PHS1** (10 μM) in presence and absence of Na_2S (200 μM) at various pH (4–9.5). The spectra were recorded in PBS buffer (pH = 7.4; 1% DMSO) at 37 °C and excitation was effected at 450 nm; both excitation and emission slit widths set at 5 nm.

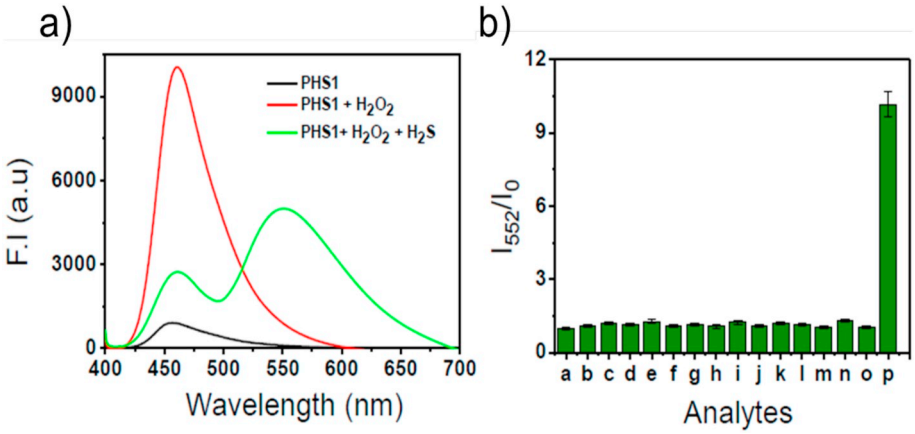

Fig. 3. a) Fluorescence intensity changes of **PHS1** (10 μM) in the absence and presence of both H_2O_2 and H_2S (200 μM) at pH (7.4). b) Fluorescence response of **PHS1** (10 μM) towards 200 μM a: HOCl, b: H_2O_2, c: $NaNO_2$, d: tyrosinase, e: K_2S_5, f: $Na_2S_2O_3$, g: $FeSO_4$, h: NO i: pepsin j: $CaCl_2$ k: NaOCl, l: GSH (1 mM), m: ascorbic Acid (1 mM), n: cysteine (1 mM), o: ALP (1 mM), p: H_2O_2 and H_2S. Experiment was executed with 1% DMSO at 37 °C with excitation at λ_{ex} = 400 nm.

S6). Also, this process is free from interference from biologically relevant analytes and pH, as fluorescence intensity of **PHS1** has remained invariable in the presence of various analytes including pH (Fig. 1c-d).

On the other hand, upon incubation of **PHS1** with H_2S (Na_2S), the UV-abs. at λ_{abs} 460 nm (Fig. S4) has increased around 32-fold and the fluorescence intensity at 550 nm has increased with rising levels of H_2S (Fig. 2a). It is obviously due to the formation of 8-aminonapthalimide derivative $\mathbf{FL_{H2S}}$ (Scheme 2, Fig. S7). **PHS1** has also shown time-dependent fluorescence enhancement and reaches saturation within 60 min in the presence of 200 μM of H_2S (Na_2S).

Notably, this H_2S sensing event is free from interference from other analytes, including pH (Fig. 2c-d). Indeed, the reactivity of **PHS1** towards H_2S is pH-dependent and showed strong fluorescence intensity within pH 6–8.5 range (Fig. 2d). By using the regression equation, the detection limit of **PHS1** towards H_2S was found to be 52.3×10^{-5} μM (Fig. S8).

We then established the crosstalk between H_2S and H_2O_2 through FRET-based fluorescence study. As depicted in Fig. 3a, a fluorescence signal at 550 nm with a small shoulder peak at 450 nm is observed in H_2S/H_2O_2 incubated **PHS1** solution while excitation was effected at 400 nm. The small peak at 450 nm indicated that the FRET mechanism is partially perturbed. This FRET-based fluorescence signal was obtained because of the formation of **FL-1** (Scheme 2); it was confirmed by HRMS analysis and ^{1}H NMR (Fig. S9–10) of H_2S/H_2O_2 pretreated **PHS1**. Notably, this crosstalk event is free from interference from other analytes (Fig. 3b). All the experimental results led us to conclude that the probe **PHS1** could detect H_2S, H_2O_2, and H_2S/H_2O_2 by providing multicolor fluorescence images in live cells.

3.2. Cell Viability and Tracking of H_2S, H_2O_2, and H_2S/H_2O_2 in Live Cells

The probe **PHS1** had shown negligible cytotoxicity at very high concentrations (≥ 50 μM) against HT29 cells, but it is nontoxic within the range of levels used for cell imaging (≤ 10 μM) (Fig. S11). Such non-toxic nature of **PHS1** encourages using it in vitro tracking of endogenous analytes, such as H_2S, H_2O_2, and H_2S/H_2O_2 respectively. Next, we had proceeded towards labeling of colon cancer cells (HT29) based on endogenous H_2S. We noticed in Fig. 4e, the cells were green

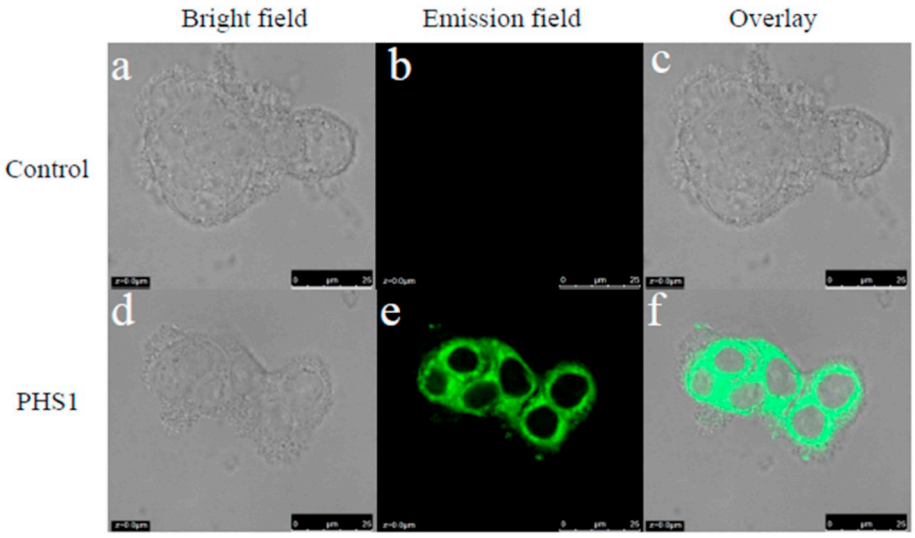

Fig. 4. Confocal fluorescence images of HT-29. (Left) Bright field, (Middle) Fluorescence and (Right) merged image. The cells were without **PHS1** (a-c) and with **PHS1** (10 μM) were incubated with for 1.30 h (d-f). Images were collected from the emission wavelength green channel (540–580 nm) at the excitation wavelength 460 nm. Scale bar = 25 μm. (For interpretation of the references to colour in this figure legend, the reader is referred to the web version of this article.)

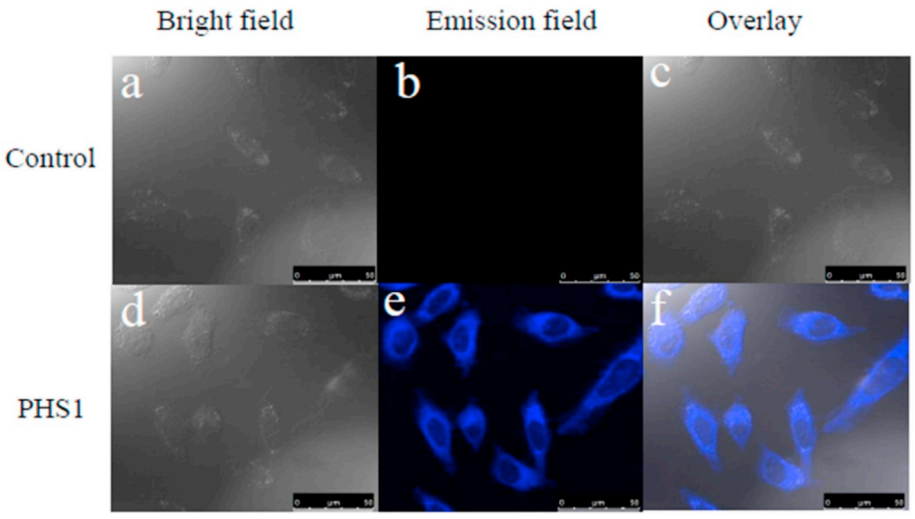

Fig. 5. Detection of PMA-induced H_2O_2 production in HeLa cells. (a-c) cells were incubated with **PHS1** (10 μM) for 30 min. (d-f) Subsequent treatment of the cells with the stimulant PMA (25 ng mL^{-1}) for 2 h. Images were collected from the emission wavelength blue channel (450–480 nm) at the excitation wavelength 400 nm. Scale bar = 50 μm. (For interpretation of the references to colour in this figure legend, the reader is referred to the web version of this article.)

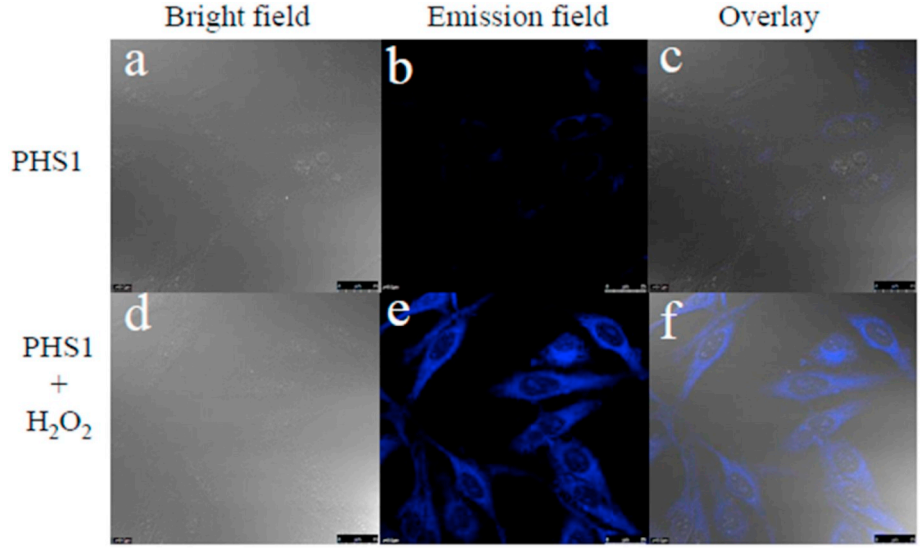

Fig. 6. Confocal fluorescence images of HeLa cells. (a-c) cells were incubated with **PHS1** (10 μM) for 30 min. (d-f) Subsequent treatment of the cells with H_2O_2 (150 μM) for 30 min. Images were collected from the emission wavelength blue channel (450–480 nm). Scale bar = 25 μm.

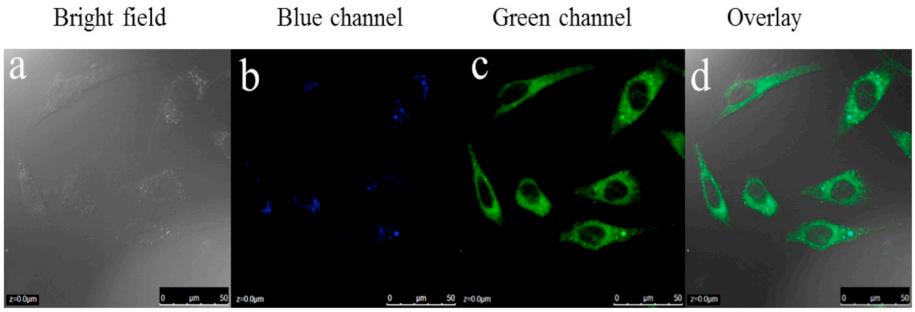

Fig. 7. Confocal fluorescence images of HeLa cells. The probe **PHS1** (10 μM) were incubated for 30 min and then treated (a-d) both H_2O_2 (200 μM) and H_2S (200 μM). Images were collected from the emission wavelength blue channel (450–480 nm) green channel (540–580 nm) at the excitation wavelength 400 nm. Scale bar = 50 μm. (For interpretation of the references to colour in this figure legend, the reader is referred to the web version of this article.)

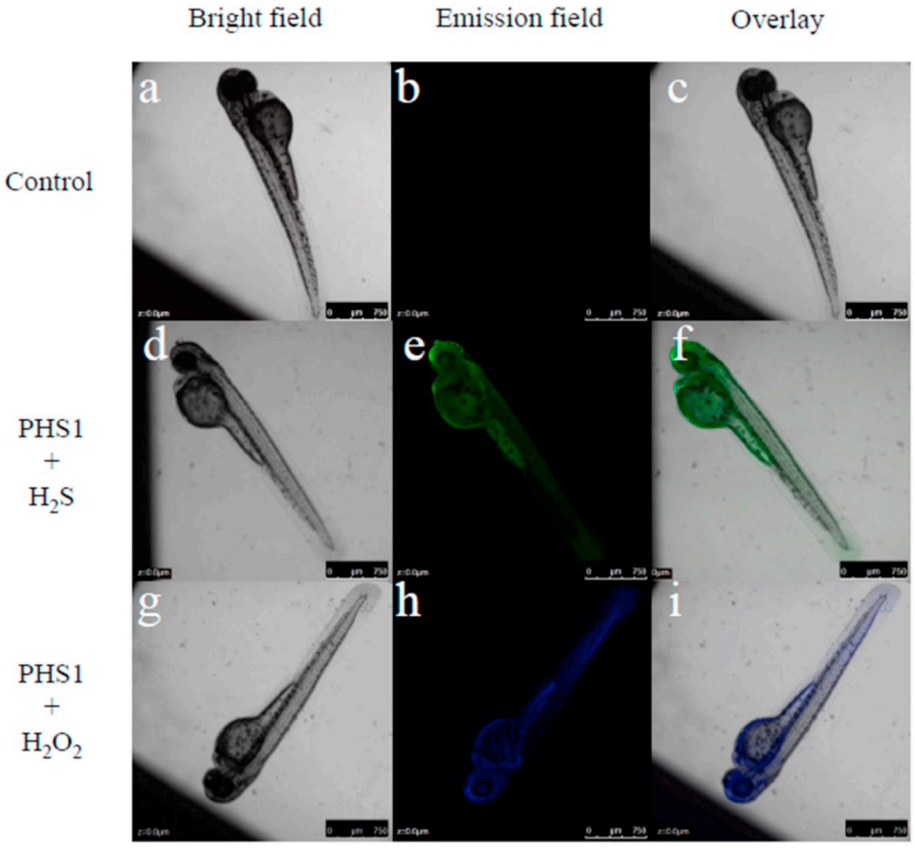

Fig. 8. Confocal microscopy images of 5-day-old zebrafish (Left) Bright field; (Middle) Fluorescence; and (Right) merged image. (a-c) the zebrafish were without **PHS1**. (d-f) the zebrafish were incubated with **PHS1** (50 μM) for 30 min and then with H_2S (150 μM) for 30 min. (g-i) the zebrafish were incubated with **PHS1** (50 μM) for 30 min and then with H_2O_2 (150 μM) for 30 min. Images were collected at the blue (450–480 nm) and green channels (540–580 nm) with 400 and 450 nm excitation, respectively. Scale bar = 750 μm. (For interpretation of the references to colour in this figure legend, the reader is referred to the web version of this article.)

fluorescence labeled upon incubation with probe **PHS1**. This green fluorescence image is because of the conversion of N_3- to H_2N- in the naphthalimide moiety of **PHS1** in the presence of endogenous H_2S [21]. On the other hand, there were no fluorescence signals either in blue or green channel upon excitation at 400 nm/450 nm in **PHS1** incubated HeLa cells; evidently, it is due to insufficient endogenous H_2O_2/H_2S formation.

3.3. Fluorescence Imaging

We were then interested in the tracking of stimulator-induced endogenous H_2O_2 formation in HeLa cells. Thus, **PHS1** pretreated HeLa cells were further incubated with phorbol 12-myristate 13-acetate (PMA) to induce endogenous H_2O_2 formation; as a result, bright fluorescence images were obtained in the blue channel (Fig. 5e). It is apparently due to the formation of endogenous H_2O_2, as noticed in the previous study [47]. Similarly, when **PHS1** was treated with exogenous H_2O_2 (150 μM) for 30 min, it provided blue fluorescence images. (Fig. 6). It indicates that the probe **PHS1** can detect both exogenous and endogenous H_2O_2 in the live cells.

We then proceed to check the presence of both H_2O_2/H_2S in cancer cells by acquiring FRET based images in the green fluorescence channel. As shown in Fig. 7, there was virtually no fluorescence in the blue channel region upon exciting at λ_{ex} 400 nm in H_2O_2/H_2S pretreated HeLa cells; instead, in the green channel marked fluorescence was noticed (Fig. 7c). These findings are well consistent with our designed strategy for tracking of H_2O_2, H_2S and H_2O_2/H_2S formation in cancer cells through multicolor fluorescence imaging. The dual analytes (H_2O_2 and H_2S) sensing in cancer cells could be a unique strategy for diagnosing cancer cells which may pave the way to develop new therapeutics in cancer treatment.

3.4. Tracking of Exogenous H_2S, and H_2O_2 in Live-Specimen

Finally, we examined the in vivo H_2O_2 and H_2S formation in the Zebrafish life specimen. As shown in Fig. 8e-f, the probe **PHS1** treated Zebrafish is labeled in green fluorescence channel in the presence of H_2S. On the other hand, Zebrafish coincubated with **PHS1**/H_2O_2 are blue fluorescence labeled (Fig. 8h-i). From this result, we can conclude that probe **PHS1** can validate both H_2O_2 and H_2S formation in the live specimen.

4. Summary and Conclusions

We described synthesis and application of FRET-based dual channel bioorthogonal fluorescent probe **PHS1** for tracking of endogenous H_2S, H_2O_2, and H_2O_2/H_2S formation in cancer cells. The discrete UV-abs and emission of coumarin and naphthalimide of **PHS1** allowed detecting dual analytes, H_2O_2/H_2S in blue and green emission channel respectively. The H_2S, H_2O_2 and H_2O_2/H_2S detection events are free from interference from other omnipresent interferants in the living cells. The green channel fluorescence images indicated that endogenous H_2S formation in colon cancer cells (HT29 cells) is higher than the cervical cancer cells (HeLa cells). We successfully confirmed endogenous H_2S, H_2O_2, and H_2O_2/H_2S formation in cancer cells through multicolor fluorescence imaging. This dual analyte-responsive strategy can overcome the inhomogeneous distribution of dual probes and enables us to provide accurate information on intracellular multi-analytes. This strategy may encourage the development of multi-analytes based fluorescence marker for labeling of cancer cells.

Acknowledgements

SB wishes to thank DST-SERB, India for a research grant (ECR/2015/000035).

Appendix A. Supplementary data

Supplementary data to this article can be found online at https://doi.org/10.1016/j.jphotobiol.2018.12.016.

References

[1] A. Banjac, T. Perisic, H. Sato, A. Seiler, S. Bannai, N. Weiss, P. Kolle, K. Tschoep, R.D. Issels, P.T. Daniel, M. Conrad, G.W. Bornkamm, The cystine/cysteine cycle: a redox cycle regulating susceptibility versus resistance to cell death, Oncogene 27 (2008) 1618–1628.
[2] L. Sullivan, N. Chandel, Mitochondrial reactive oxygen species and cancer, Cancer Metab. 2 (2014) 17 (1–12.
[3] K.M. Holmstrom, T. Finkel, Cellular mechanisms and physiological consequences of redox-dependent signalling, Nat. Rev. Mol. Cell Biol. 15 (2014) 411–421.
[4] C.E. Paulsen, K.S. Carroll, Cysteine-mediated redox signaling: chemistry, biology, and tools for discovery, Chem. Rev. 113 (2013) 4633–4679.
[5] M. Reth, Hydrogen peroxide as second messenger in lymphocyte activation, Nat. Immun. 3 (2002) 1129–1134.
[6] R.D. Balsara, V.A. Ploplis, Plasminogen activator inhibitor-1: the double-edged sword in apoptosis, Thromb. Haemost. 100 (2008) 1029–1036.
[7] S. Benedetti, B. Nuvoli, S. Catalani, R. Galati, Reactive oxygen species a double-edged sword for mesothelioma, Oncotarget 6 (2015) 16848–16865.
[8] A.R. Lippert, G.C. Van de Bittner, C.J. Chang, Boronate oxidation as a bioorthogonal reaction approach for studying the chemistry of hydrogen peroxide in living systems, Acc. Chem. Res. 44 (2011) 793–804.
[9] F.G. Giancotti, Deregulation of cell signaling in cancer, FEBS Lett. 588 (2014) 2558–2570.
[10] R. Sever, J.S. Brugge, Signal transduction in cancer, Cold Spring Harb. Perspect. Med. 5 (2015) a006098(1 − 21).
[11] R. Wang, Physiological implications of hydrogen sulfide: a whiff exploration that blossomed, Physiol. Rev. 92 (2012) 791–896.
[12] D.J. Lefer, A new gaseous signaling molecule emerges: cardioprotective role of hydrogen sulfide, Proc. Natl. Acad. Sci. U. S. A. 46 (2007) 17907–17908.
[13] K. Modis, E.M. Bos, E. Calzia, H. van Goor, C. Coletta, A. Papapetropoulos, M.R. Hellmich, P. Radermacher, F. Bouillaud, C. Szabo, Regulation of mitochondrial bioenergetic function by hydrogen sulfide. Part II. Pathophysiological and therapeutic aspects, Br. J. Pharmacol. 171 (2014) 2123–2146.
[14] Y.J. Peng, J. Nanduri, G. Raghuraman, D. Souvannakitti, M.M. Gadalla, G.K. Kumar, S.H. Snyder, N.R. Prabhakar, H_2S mediates O_2 sensing in the carotid body, Proc. Natl. Acad. Sci. U. S. A. 107 (2010) 10719–10724.
[15] A. Papapetropoulos, A. Pyriochou, Z. Altaany, G. Yang, A. Marazioti, Z. Zhou, M.G. Jeschke, L.K. Branski, D.N. Herndon, R. Wang, C. Szabo, Hydrogen sulfide is an endogenous stimulator of angiogenesis, Proc. Natl. Acad. Sci. U. S. A. 106 (2009) 21972–21977.
[16] C. Szabo, A. Papapetropoulos, Hydrogen sulphide and angiogenesis: mechanisms and applications, Br. J. Pharmacol. 164 (2011) 853–865.
[17] A.K. Mustafa, G. Sikka, S.K. Gazi, J. Steppan, S.M. Jung, A.K. Bhunia, V.M. Barodka, F.K. Gazi, R.K. Barrow, R. Wang, L.M. Amzel, D.E. Berkowitz, S.H. Snyder, Hydrogen sulfide as endothelium-derived hyperpolarizing factor sulfhydrates potassium channels, Circ. Res. 109 (2011) 1259.
[18] H. Kimura, Hydrogen sulfide: its production, release and functions, Amino Acids 41 (2011) 113–121.
[19] Y. Zhou, K.N. Bobba, X.W. Lv, D. Yang, N. Velusamy, J.F. Zhang, S. Bhuniya, A biotinylated piperazine-rhodol derivative: a 'turn-on' probe for nitroreductase triggered hypoxia imaging, Analyst 142 (2017) 345–350.
[20] K.N. Bobba, G. Saranya, S.M. Alex, N. Velusamy, K.K. Maiti, S. Bhuniya, SERS-active multi-channel fluorescent probe for NO: Guide to discriminate intracellular biothiols, Sensors Actuators B Chem. 260 (2018) 165–173.
[21] K. Sunwoo, K.N. Bobba, J.Y. Lim, T. Park, A. Podder, J.S. Heo, S.G. Lee, S. Bhuniya, J.S. Kim, A bioorthogonal 'turn-on' fluorescent probe for tracking mitochondrial nitroxyl formation, Chem. Commun. 53 (2017) 1723–1726.
[22] K.N. Bobba, Y. Zhou, L.E. Guo, T.N. Zang, J.F. Zhang, S. Bhuniya, Resorufin based fluorescence 'turn-on' chemodosimeter probe for nitroxyl (HNO), RSC Adv. 5 (2015) 84543–84546.
[23] A. Podder, S. Senapati, P. Maiti, D. Kamalraj, S.S. Jaffer, S. Khatun, S. Bhuniya, A 'turn-on' fluorescent probe for lysosomal phosphatase: a comparative study for labeling of cancer cells, J. Mater. Chem. B 6 (2018) 4514–4521.
[24] E.J. Kim, S. Bhuniya, H. Lee, H.M. Kim, C. Cheong, S. Maiti, K.S. Hong, J.S. Kim, An activatable prodrug for the treatment of metastatic tumors, J. Am. Chem. Soc. 136 (2014) 13888–13894.
[25] X. Han, X. Song, B. Li, F. Yu, L. Chen, A near-infrared fluorescent probe for sensitive detection and imaging of sulfane sulfur in living cells and in vivo, Biomater. Sci. 6 (2018) 672–682.
[26] X. Song, X. Han, F. Yu, J. Zhang, L. Chen, C. Lv, A reversible fluorescent probe based on C[double bond, length as m-dash]N isomerization for the selective detection of formaldehyde in living cells and in vivo, Analyst 143 (2018) 429–439.
[27] Y. Chen, X. Shi, Z. Lu, X. Wang, Z. Wang, A fluorescent probe for hydrogen peroxide in vivo based on the modulation of intramolecular charge transfer, Anal. Chem. 89 (2017) 5278–5284.
[28] M. Abo, Y. Urano, K. Hanaoka, T. Terai, T. Komatsu, T. Nagano, Development of a highly sensitive fluorescence probe for hydrogen peroxide, J. Am. Chem. Soc. 133 (2011) 10629–10637.
[29] B.C. Dickinson, C.J. Chang, A targetable fluorescent probe for imaging hydrogen peroxide in the mitochondria of living cells, J. Am. Chem. Soc. 130 (2008) 9638–9639.
[30] C. Gao, Y. Tian, R. Zhang, J. Jing, X. Zhang, Endoplasmic reticulum-directed ratiometric fluorescent probe for quantitive detection of basal H_2O_2, Anal. Chem. 89 (2017) 12945–12950.
[31] H. Xiao, P. Li, X. Hu, X. Shi, W. Zhang, B. Tang, Simultaneous fluorescence imaging of hydrogen peroxide in mitochondria and endoplasmic reticulum during apoptosis, Chem. Sci. 7 (2016) 6153.
[32] J. Hou, M. Qian, H. Zhao, H.Y. Li, Y. Liao, G. Han, Z. Xu, F. Wang, Y. Song, Y. Liu, A near-infrared ratiometric/turn-on fluorescent probe for in vivo imaging of hydrogen peroxide in a murine model of acute inflammation, Anal. Chim. Acta 1024 (2018) 169.
[33] N. Zhang, B. Dong, X. Kong, C. Wang, W. Song, W. Lin, Development of a xanthene-based red-emissive fluorescent probe for visualizing H2O2 in living cells, tissues and animals, J. Fluoresc. 28 (2018) 681–687.
[34] D. Kim, G. Kim, S.J. Nam, J. Yin, J. Yoon, Visualization of endogenous and exogenous hydrogen peroxide using a lysosome-targetable fluorescent probe, Sci. Rep. 5 (2015) 8488.
[35] Y. Hitomi, Y.T. Takeyasu, T. Funabiki, M. Kodera, Detection of enzymatically generated hydrogen peroxide by metal-based fluorescent probe, Anal. Chem. 83 (2011) 9213–9216.
[36] M.D. Hammers, M.J. Taormina, M.M. Cerda, L.A. Montoya, D.T. Seidenkranz, R. Parthasarathy, M.D. Pluth, J. Am. Chem. Soc. 137 (2015) 10216–10223.
[37] B. Gu, W. Su, L. Huang, C. Wu, X. Duan, Y. Li, H. Xu, Z. Huang, H. Li, S. Yao, Real-time tracking and selective visualization of exogenous and endogenous hydrogen sulfide by a near-infrared fluorescent probe, Sensors Actuators B Chem. 255 (2018) 2347–2355.
[38] J. Cui, T. Zhang, Y.Q. Sun, D.P. Li, J.T. Liu, B.X. Zhao, A highly sensitive and selective fluorescent probe for H_2S detection with large fluorescence enhancement, Sensors Actuators B Chem. 232 (2016) 705–711.
[39] N. Velusamy, A. Binoy, K.N. Bobba, D. Nedungadi, N. Mishra, S. Bhuniya, A bioorthogonal fluorescent probe for mitochondrial hydrogen sulfide: new strategy for cancer cell labeling, Chem. Commun. 53 (2017) 8802–8805.
[40] W. Sun, J. Fan, C. Hu, J. Cao, H. Zhang, X. Xiong, J. Wang, S. Cui, S. Sun, X. Peng, A two-photon fluorescent probe with near-infrared emission for hydrogen sulfide imaging in biosystems, Chem. Commun. 49 (2013) 3890–3892.
[41] S. Nandi, H. Reinsch, S. Banesh, N. Stock, V. Trivedi, S. Biswas, Rapid and highly sensitive detection of extracellular and intracellular H_2S by an azide-functionalized Al(iii)-based metal-organic framework, Dalton Trans. 46 (2017) 12856–12864.
[42] N. Thirumalaivasan, P. Venkatesan, S.P. Wu, Highly selective turn-on probe for H_2S with imaging applications in vitro and in vivo, New J. Chem. 41 (2017) 13510–13515.
[43] F. Chen, D. Han, H. Liu, S. Wang, K.B. Li, S. Zhang, W. Shi, A tri-site fluorescent probe for simultaneous sensing of hydrogen sulfide and glutathione and its bioimaging applications, Analyst 143 (2018) 440–448.
[44] S. Yang, Y. Qi, C. Liu, Y. Wang, Y. Zhao, L. Wang, J. Li, W. Tan, R. Yang, Design of a simultaneous target and location-activatable fluorescent probe for visualizing hydrogen sulfide in lysosomes, Anal. Chem. 86 (2014) 7508–7515.
[45] A. AH, S. Sreedharan, F. Ali, C.G. Smythe, J.A. Thomas, A. Das, Polysulfide-triggered fluorescent indicator suitable for super-resolution microscopy and application in imaging, Chem. Commun. 54 (2018) 3735–3738.
[46] V.S. Lin, A.R. Lippert, C.J. Chang, Cell-trappable fluorescent probes for endogenous hydrogen sulfide signaling and imaging H_2O_2-dependent H_2S production, Proc. Natl. Acad. Sci. U. S. A. 110 (2013) 7131–7135.
[47] A. Podder, M. Wonb, S. Kimb, P. Verwilstb, M. Maiti, Z. Yang, J. Quc, S. Bhuniya, J.S. Kim, A two-photon fluorescent probe records the intracellular pH through 'OR' logic operation via internal calibration, Sensors Actuators B Chem. 268 (2018) 195–204.
[48] L. He, W. Lin, Q. Xu, H. Wei, A new strategy to construct a FRET platform for ratiometric sensing of hydrogen sulfide, Chem. Commun. 51 (2015) 1510–1513.